Migration of Motor Pool Activity in the Spinal Cord Reflects Body Mechanics in Human Locomotion

Germana Cappellini, Yuri P. Ivanenko, Nadia Dominici, Richard E. Poppele and Francesco Lacquaniti

J Neurophysiol 104:3064-3073, 2010. First published 29 September 2010; doi:10.1152/jn.00318.2010

J Neurophysiol 104: 3064–3073, 2010.
First published September 29, 2010; doi:10.1152/jn.00318.2010.

Migration of Motor Pool Activity in the Spinal Cord Reflects Body Mechanics in Human Locomotion

Germana Cappellini,[1] Yuri P. Ivanenko,[1] Nadia Dominici,[1,2] Richard E. Poppele,[4] and Francesco Lacquaniti[1,2,3]
[1]*Laboratory of Neuromotor Physiology, Santa Lucia Foundation;* [2]*Centre of Space Bio-medicine and* [3]*Department of Neuroscience, University of Rome Tor Vergata, Rome, Italy; and* [4]*Department of Neuroscience, University of Minnesota, Minneapolis, Minnesota*

Submitted 6 April 2010; accepted in final form 23 September 2010

Cappellini G, Ivanenko YP, Dominici N, Poppele RE, Lacquaniti F. Migration of motor pool activity in the spinal cord reflects body mechanics in human locomotion. *J Neurophysiol* 104: 3064–3073, 2010. First published September 29, 2010; doi:10.1152/jn.00318.2010. During the evolution of bipedal modes of locomotion, a sequential rostrocaudal activation of trunk muscles due to the undulatory body movements was replaced by more complex and discrete bursts of activity. Nevertheless, the capacity for segmental rhythmogenesis and the rostrocaudal propagation of spinal cord activity has been conserved. In humans, motoneurons of different muscles are arranged in columns, with a specific grouping of muscles at any given segmental level. The muscle patterns of locomotor activity and the biomechanics of the body center of mass have been studied extensively, but their interrelationship remains poorly understood. Here we mapped the electromyographic activity recorded from 30 bilateral leg muscles onto the spinal cord in approximate rostrocaudal locations of the motoneuron pools during walking and running in humans. We found that the rostrocaudal displacements of the center of bilateral motoneuron activity mirrored the changes in the energy due to the center-of-body mass motion. The results suggest that biomechanical mechanisms of locomotion, such as the inverted pendulum in walking and the pogo-stick bouncing in running, may be tightly correlated with specific modes of progression of motor pool activity rostrocaudally in the spinal cord.

INTRODUCTION

The basic activity pattern for locomotion is generated by neuronal networks referred to as central pattern generators, whose activity also depends on descending and sensory afferent signals (Orlovsky et al. 1999). Locomotor patterns are highly adaptable to changes in the environment (Cappellini et al. 2006; Clarac et al. 2004; Ivanenko et al. 2009; Nilsson et al. 1985). The actual output of central pattern generators (Grillner 2006) and optimization of human gaits may be directly related to the biomechanics of body movement and, in particular, to the dynamics of limb loading and center-of-body-mass (COM) motion (Alexander 1989; Lacquaniti et al. 1999, 2002; Saibene and Minetti 2003). According to the inverted-pendulum analogy, COM (located close to the hips) vaults over the stance limb while the contralateral limb swings in a synchronized fashion (Alexander 1989). The control of the COM through appropriate intersegmental coordination is instrumental for saving the mechanical energy of the body (Bianchi et al. 1998; Massaad et al. 2007). Running, instead, can be described as a sequence of parabolic free-flight arcs, with impulses from the ground at each bounce (Alexander 1989; Bramble and Lieberman 2004; Cavagna et al. 1976; Saibene and Minetti 2003). The COM trajectory curves upward during the stance phase of walking in humans whereas it curves downward in running, reflecting a major functional difference for the support limb, which tends to act more like a rigid strut in walking and like a spring in running. The literature on the pendulum mechanism of walking and bouncing mechanism in running in different animals has been growing rapidly in recent years (see, for instance, Ivanenko et al. 2007; Massaad et al. 2007; Saibene and Minetti 2003; Srinivasan and Ruina 2006). However, their neural substrates or correlates remain poorly understood. What is the relationship between spinal cord activity and the biomechanics of bipedal gait?

α-Motoneurons (MNs) in the human spinal cord show a very specific topography (Kendall et al. 1993; Sharrard 1964). In general, each muscle is innervated by several spinal segments and each segment supplies several muscles. Such anatomical grouping may reflect basic functioning of leg muscles during terrestrial locomotion. However, no previous study has specifically addressed this question, except for a few studies on a rostrocaudal propagation of motor waves in trunk muscles (de Sèze et al. 2008; Falgairolle et al. 2006). Recently, a new approach was developed for cats (Yakovenko et al. 2002) and humans (Ivanenko et al. 2006) that represents a viable technique for documenting the spatiotemporal maps of MNs. It consists of simultaneous kinematic and electromyographic (EMG) recordings in several muscles and mapping the recorded patterns of muscle activity onto the approximate rostrocaudal location of the MN pools in the human spinal cord. Spinal segmental localization charts are created by integrating anatomical and clinical data from several different sources (Kendall et al. 1993). This approach can be used to characterize network architecture for different gaits by considering relative intensities, spatial extent, and temporal structure of the spinal motor output (Bonnet et al. 2002; Cuellar et al. 2009; Falgairolle et al. 2006; Golubitsky et al. 1999; Ivanenko et al. 2008; Mentel et al. 2008).

Here we investigated the spinal motor output and its relation to the biomechanics of walking and running. We focused on the lumbosacral enlargement because it contains the MNs of all the leg muscles. Ipsilateral maps of activation have been previously reported (Cappellini et al. 2010; Ivanenko et al. 2006, 2008). However, in this study we analyzed for the first time the bilateral spinal cord output and its relation to the mechanics of the body center of mass. In this analysis, the activity of the left and right leg muscles was collapsed within one gait cycle defined for the right leg. The rationale for the bilateral analysis is that the COM motion of the body is determined by coordinated activity of all muscles of both legs

Address for reprint requests and other correspondence: Y. P. Ivanenko, Laboratory of Neuromotor Physiology, IRCCS Fondazione Santa Lucia, 306 via Ardeatina, 00179 Rome, Italy (E-mail: y.ivanenko@hsantalucia.it).

rather than by muscles of only one leg. We found a striking correspondence of the rostrocaudal propagation of spinal cord activity with changes in the energy of the COM motion, suggesting a possible neural underpinning of the biomechanics of bipedal gait.

METHODS

A total of 15 healthy subjects (age range between 25 and 47 yr; 11 males, 4 females) were enrolled in this study. None of the subjects had any history of neurological or orthopedic disease. Informed consent was obtained from all participants. The studies conformed to the Declaration of Helsinki and informed consent was obtained from all participants according to the procedures of the Ethics Committee of the Santa Lucia Foundation.

The following conditions were included: walking and running on a treadmill (with the shoes on) at 3 and 9 km/h, respectively, and backward walking at 3 km/h. In addition, we also analyzed the data obtained during walking under low friction conditions (Cappellini et al. 2010): six subjects were asked to walk on either a normal or a slippery surface (7 m long, 1 m wide, using oil; the floor was protected by a polyethylene pellicle, 0.07 mm thickness) at a natural speed (on average 2.8 ± 0.5 km/h). Participants wore shoe covers over their bare feet that were made from the same thin polypropylene material used for the floor to reduce the interface friction. The operational dynamic coefficient of friction was 0.06 ± 0.01 (Cappellini et al. 2010). Thirteen consecutive trials of walking on the slippery surface were recorded in each subject.

Because the methods have been thoroughly documented in our previous studies (Cappellini et al. 2006; Ivanenko et al. 2006, 2008), here we describe only briefly the experimental measurements and analysis. Kinematic data were recorded bilaterally at 100 Hz by means of the Vicon-612 system (Oxford Metrics, Oxford, UK). Nine TV cameras were spaced around the walkway. Infrared reflective markers (1.4 cm diameter) were attached on each side of the subject to the skin overlying the following landmarks: glenohumeral joint, elbow, wrist, ilium, greater trochanter, lateral femur epicondyle, lateral malleolus, heel, and fifth metatarsophalangeal joint. The gait cycle was defined with respect to the right leg movement, beginning with right foot contact with the surface, according to the local minima of the vertical displacement of the heel (for forward walking) or fifth metatarsophalangeal joint (for backward walking) marker (Ivanenko et al. 2008). The timing of the liftoff was determined similarly (when the fifth metatarsophalangeal joint marker was raised by 3 cm). The touchdown events were verified from the force plate recordings in our previous studies and we found that the kinematic criteria we used predicted the onset of stance phase with an error <2% of the gait cycle duration (Cappellini et al. 2006).

Electromyographic activity was recorded by means of surface electrodes (model DE2.1; Delsys, Boston, MA) from 30 bilateral muscles simultaneously. The following 15 muscles were recorded from each body side: tibialis anterior (TA), gastrocnemius lateralis (LG), gastrocnemius medialis (MG), soleus (SOL), peroneus longus (PERL), vastus lateralis (VL), vastus medialis (VM), rectus femoris (RF), sartorius (SART), biceps femoris (long head, BF), semitendinosus (ST), adductor longus (ADD), tensor fascia latae (TFL), gluteus maximus (GM), and gluteus medius (Gmed). Electrode placement was carefully chosen (Cappellini et al. 2006; Kendall et al. 1993) to minimize cross talk from adjacent muscles during isometric contractions. The signals were amplified, filtered (20–450 Hz) (Bagnoli 16; Delsys), and sampled at 1,000 Hz. Samplings of kinematic and EMG data were synchronized. The EMG records were numerically rectified, low-pass filtered using a zero-lag fourth-order Butterworth filter with a cutoff of 10 Hz, time-interpolated over individual gait cycles to fit a normalized 200-point time base, and averaged across steps to obtain the ensemble-averaged EMG patterns.

At the end of the recording session, anthropometric measurements were taken on each subject. These included the mass and stature of the subject and both the length and the circumference of the main segments of the body (Cappellini et al. 2010).

Kinetic and potential energies of the COM

Potential and kinetic energies of the center of body mass were estimated by computing its instantaneous position and velocity. COM position was derived as

$$COM = \frac{\sum_{i}^{n} m_i \cdot \vec{r}_i}{\sum_{i}^{n} m_i} \quad (1)$$

where m_i and $\vec{r}_i$ are the mass and position of the center of mass of each body segment (11 segments total: bilateral thigh, shank, foot, arm, forearm, and trunk head), respectively, derived using measured kinematics, anthropometric data taken on each subject (see preceding text), and regression equations proposed for adults (Cappellini et al. 2010). The potential (E_p) and kinetic (E_k) energies of the COM were computed according to the following equations

$$E_p = mgh \quad (2)$$

$$E_k = ½mV^2 \quad (3)$$

where m is the body mass, h is the vertical position of the COM, and V is its forward velocity in the sagittal plane. The classical analysis of the inverted pendulum involves only sagittal components of body motion (Cavagna et al. 1976; Saibene and Minetti 2003) since it has been shown that the lateral component of kinetic energy of the COM is essentially negligible compared with that of the sagittal components (Cappellini et al. 2010; Tesio et al. 1998).

Spatiotemporal patterns of MN activity in the spinal cord

The recorded patterns of EMG activity were mapped onto the approximate rostrocaudal location of MN pools in the human spinal cord (Ivanenko et al. 2006). In this study we used two myotomal charts: those of Kendall et al. (1993) and of Sharrard (1964). Table 1 shows Kendall's chart of innervation of leg muscles, whose activity was recorded in the current study, and Fig. 1, which illustrates the

TABLE 1. *Muscle innervation as depicted on a Kendall chart*

	GM	Gmed	TFL	SART	ADD	RF	Vlat	Vmed	BF	ST	LG	MG	SOL	PERL	TA
L2				X	X	X	X	X							
L3				X	X	X	X	X							
L4		X	X		x	X	X	X		x				x	X
L5	X	X	X						x	X			x	X	X
S1	X	X	X						X	X	X	X	X	X	X
S2	X								X	X	X	X	X		

Adapted from Kendall et al. (1993).

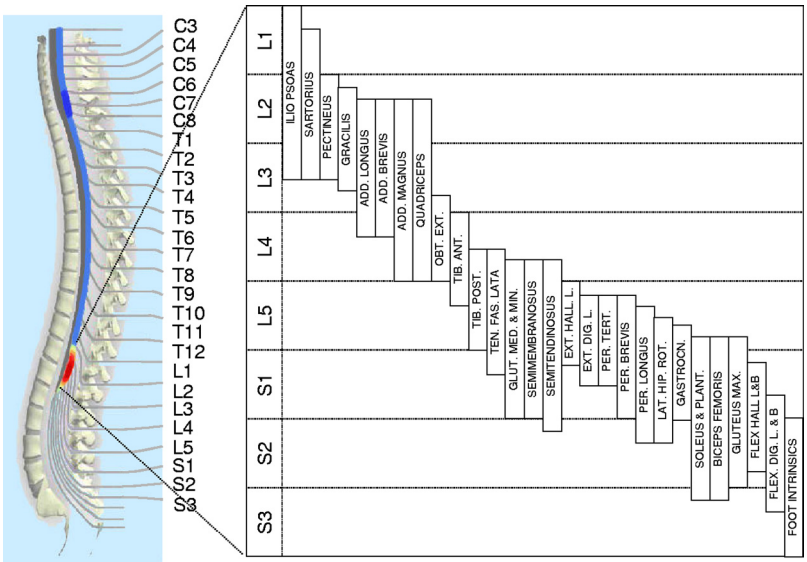

FIG. 1. Innervation of the lower limb muscles from the lumbosacral enlargement. Results redrawn from Sharrard (1964).

Sharrard data table that approximates the proportion of total muscle activation attributable to each segment of the lumbosacral enlargement. Kendall and colleagues compiled reference segmental charts for all body muscles by combining the anatomical and clinical data from six different sources. A capital X in Kendall's chart denotes localization agreed on by five or more sources, a lowercase x denotes agreement of three to four sources, and a lowercase x in parentheses (x) denotes agreement of only two sources. In our maps, X and x were weighted 1.0 and 0.5, respectively, whereas we discarded (x). We assumed that our population of subjects has the same spinal topography as this reference population.

To reconstruct the output pattern of any given spinal segment *Sj* of the most active lumbosacral segments (L2–S2), all rectified EMG waveforms corresponding to that segment were averaged. The assumption implicit in this method is that the rectified EMG provides an indirect measure of the net firing of MNs of that muscle. We used the nonnormalized procedure (EMGs were expressed in microvolts [μV]; Ivanenko et al. 2008)

$$S_j = \frac{\sum_{i=1}^{n_j} k_{ij} \cdot EMG_i}{n_j} \quad (4)$$

where n_j is the number of EMG_i waveforms corresponding to the jth segment and k_{ij} is the weighting coefficient for the ith muscle (X and x in Kendall's chart were weighted with $k_{ij} = 1.0$ and $k_{ij} = 0.5$, respectively). Sensitivity of the method to different normalization procedures was also assessed (see following text).

Using the Kendall chart results in the six rostrocaudal (L2–S2) discrete activation waveforms (Fig. 2, blue curves). To visualize a continuous smoothed rostrocaudal spatiotemporal activation of the spinal cord we used a filled contour plot that computes isolines calculated from the activation waveform matrix (6 segments × 200

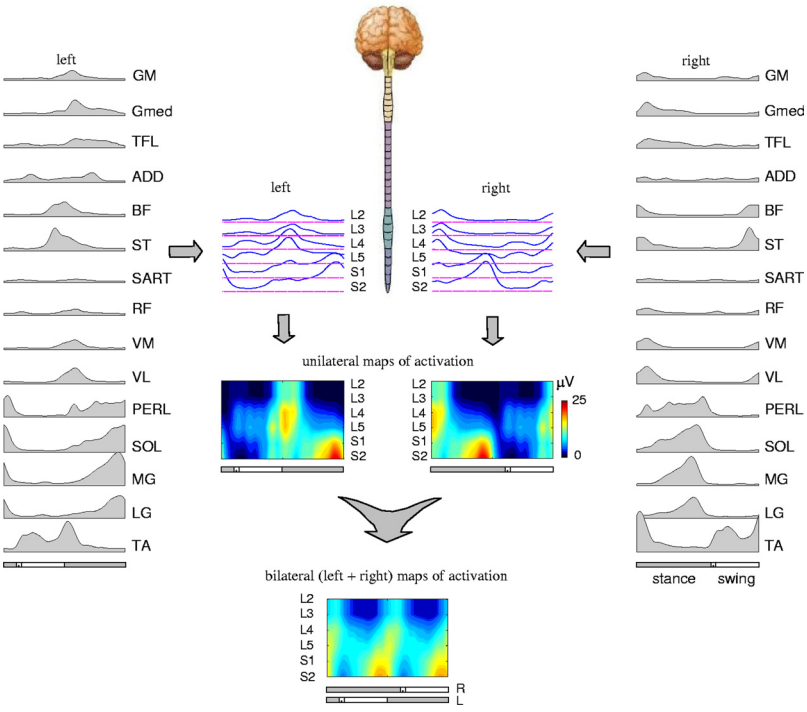

FIG. 2. Spatiotemporal patterns of α-motoneuron (MN) activity along the rostrocaudal axis of the spinal cord during walking on a treadmill at 3 km/h. Output pattern of each segment of each side of the lumbosacral enlargement (blue curves) was reconstructed by mapping the recorded electromyographic (EMG) waveforms (nonnormalized method) onto the known charts of segmental localization (Kendall charts, Table 1). Same pattern is plotted in a color scale (right calibration bar) using a filled contour plot (*middle*). Patterns are plotted vs. the normalized gait cycle (beginning from the heel strike of the right leg). Patterns of each half cord activation (*middle*) were collapsed together to obtain the total bilateral motor output (*bottom*). R, right; L, left.

points) and fills the areas between the isolines using constant colors (the "contourf.m" function in Matlab; The MathWorks, Natick, MA).

The Kendall chart indicates only the segments innervating each muscle and not the fraction of total motor pool of the muscle that can be assigned to a segment. To verify how sensitive the reconstructed maps were to specific anatomical localizations for various muscles, we also used the Sharrard (1964) data table for innervation (Fig. 1), which approximates the proportion of total muscle activation attributable to each segment (by taking multiple slices within each spinal segment), instead of assuming equal proportions in all segments. To this end, we subdivided each segment (Fig. 1) into six subsegments and applied the same *Eq. 4* for each *j*th subsegment (Ivanenko et al. 2006). The resulting spinal cord maps of activation were not smoothed as in the case of the Kendall chart but instead they contained 36 discrete bands (6 subsegments × 6 segments; C2–L2).

To assess sensitivity of the reconstructed maps of MN activation, we compared different normalization procedures: nonnormalized (EMGs were expressed in μV) and normalized to the physiological cross-sectional area (PCSA) of leg muscles (Ward et al. 2009). In the latter case, the contribution of each muscle to the estimated activity of the *j*th segment (*Eq. 4*) was multiplied by its PCSA. In addition, we also assessed parametric sensitivity of the method to a relative contribution of different muscle groups, similarly to the procedure used by Yakovenko et al. (2002). Although the classification of muscles is somewhat ambiguous (e.g., biarticular muscles like hamstring or rectus femoris can be considered as extensors/flexors for the hip joint and flexors/extensors for the knee joint), we subdivided our muscles into the three groups according to their "dominant" action (Dostal et al. 1986): extensors (SOL, LG, MG, VL, VM, RF, GM), flexors (TA, BF, ST), and "frontal plane" muscles (ADD, TFL, Gmed, SART, PERL).

The activity of the left and right leg muscles was pooled together within one gait cycle defined for the right leg (Fig. 3) so that only the rostrocaudal dimension is considered (no spatial information is considered in the lateral or dorsoventral location of motor pools) (Fig. 2). As we indicated earlier, the rationale for this bilateral analysis is that the COM motion is determined by coordinated activity of all muscles of both legs. The temporal locus of MN activity in the lumbosacral spinal cord was estimated using a method similar to that used for the cat (Yakovenko et al. 2002). We calculated the center of activity (CoA) of the six (from L2 to S2) most active lumbosacral segments using the following equation

$$CoA = \frac{\sum_{j=1}^{N} S_j \times \vec{j}}{\sum_{j=1}^{N} S_j} \quad (5)$$

where S_j is the estimated activity (from *Eq. 4*) of the *j*th segment (the origin for the CoA and for the vector *j* being defined as the caudalmost segment) and N is the number of segments ($N = 6$ for the Kendall charts and $N = 36$ for the Sharrard charts). Thus the center of activity was expressed in terms of absolute position within the lumbosacral enlargement. The data analysis and spinal MN activity map construction were performed with software written in Matlab (R2008; The MathWorks).

RESULTS

Parametric sensitivity of the motor pool output reconstruction

Based on the recorded EMG patterns from each leg (Fig. 3) we reconstructed the total bilateral motor output of the lumbosacral enlargement during different human gaits. The data were analyzed and plotted as a function of the normalized gait cycle and the activity values of the left and right leg muscles were collapsed within one gait cycle defined for the right leg (Fig. 4). Since the spatiotemporal maps of MN activity are based on indirect measurements, we assessed the parametric sensitivity of the method to different normalization techniques and variations in the relative contribution of different muscle groups.

Figure 4*A* shows sensitivity of the method to different normalization procedures. Three methods are illustrated as follows: *1*) nonnormalized method (EMGs were expressed in μV) using Kendall charts, *2*) normalized (to PCSA) method using Kendall charts, and *3*) normalized method using Sharrard charts. Positions of the center of mass of MN activity were calculated at each time of the step cycle (black curves). Note that the change in behavior of CoA is similar when using different normalization techniques. To quantify the extent of similarity, we computed the correlation coefficients between the CoA when using the nonnormalized method (Kendall chart) and the CoA when using the normalization methods. The correlation coefficients were very high (on average 0.97 ± 0.3) for walking, running, and backward walking (correlation coefficients for the slippery surface were not calculated since the CoA displacements were small and inconsistent across subjects).

Figure 4*B* illustrates the parametric sensitivity of the CoA displacements to variations in assumed activation patterns of different muscle groups. Three parametric variations are illustrated in the relative level of MN recruitment in extensor, flexor, and "frontal plane" muscles. Again, the main effect of variations was to slightly alter the net rostrocaudal displacements (amplitude) of the CoA rather than its temporal profile. An amplified contribution of the extensor muscles (Fig. 4*B*, *left*) typically resulted in augmented CoA oscillations (cf. Fig. 4*A*, *middle* with Fig. 4*B*, *left*), indicating the major contribution of extensor muscles to the observed rostrocaudal displacements of the total motor pool activity. The relationship between these systematic displacements and the biomechanics of human gaits is considered in the following section.

COM motion and CoA migration in different gaits

Figure 5*A* illustrates changes in the mechanical energy of the COM during walking and running. The pattern is plotted versus normalized gait cycle. As previously described (Cavagna et al. 1976), gravitational potential energy E_p and forward kinetic energy E_k show out-of-phase and in-phase behavior during human walking and running, respectively. This is consistent with the representation of walking by vaulting (inverted pendulum) and running by a "bouncing" gait (leg spring-loaded behavior during stance) (Fig. 5*C*).

The total spatiotemporal activation of the lumbosacral enlargement resulting from bilateral activation is plotted in Fig. 5*B*. During walking and running, there were two major activation oscillations associated with the two heel strike events and the center of activity (CoA) demonstrated clear gait-dependent behavior. During walking, the CoA shifts caudally to the L5–S2 segments at the end of stance for each leg, resulting in a prolonged burst of sacral activity with peaks at 42 and 92% of gait cycle (Fig. 5*B*, *left*). This is mainly associated with EMG activity in ankle plantar-flexors, providing support moment and forward thrust, and the braking function of hamstring muscles of the contralateral leg. Just before heel strike, at the time of transition between stance and swing, the CoA shifts rostrally toward the upper lumbar segments. This MN

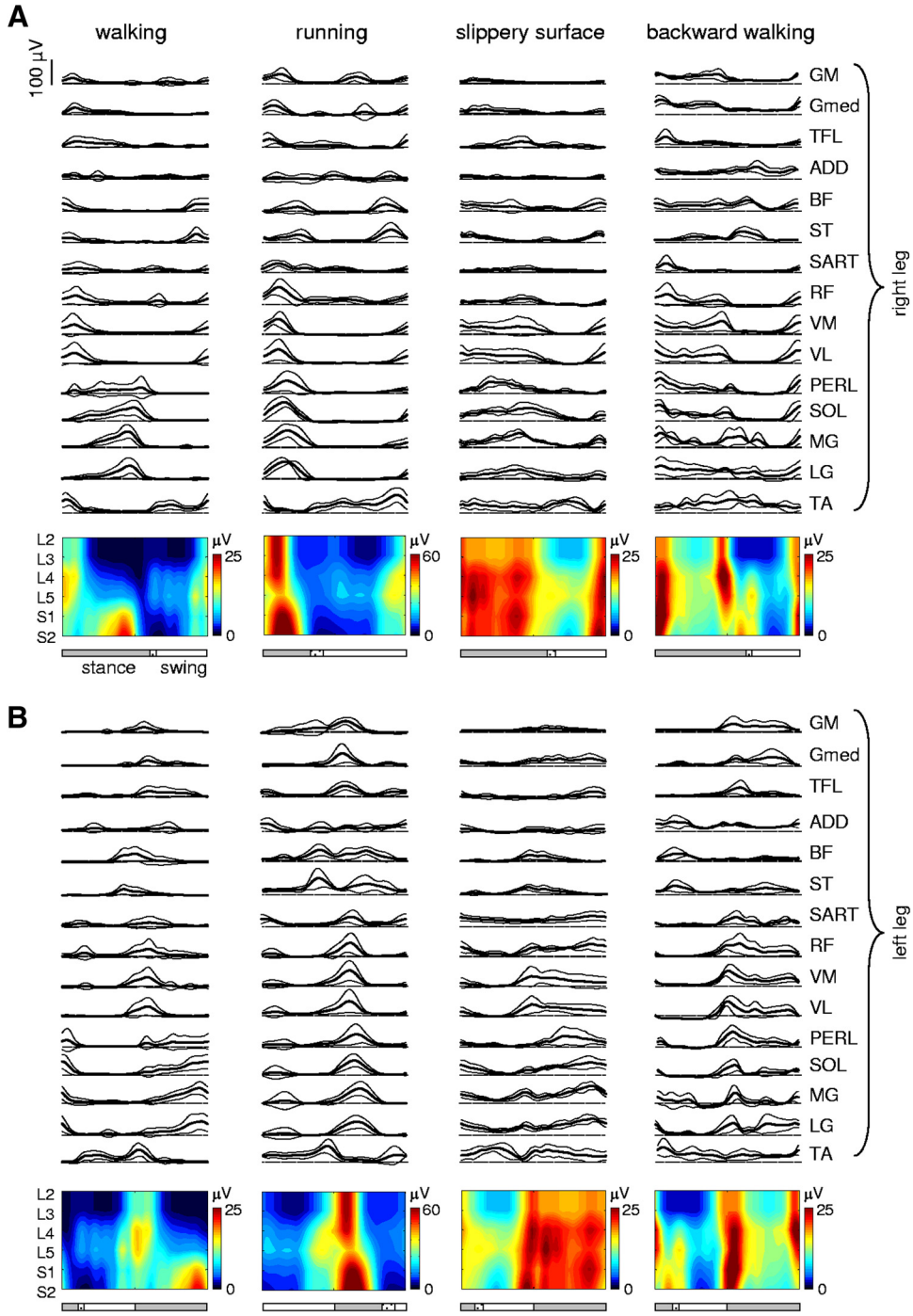

FIG. 3. Ensemble-averaged (±SD) patterns of EMG activity during walking (3 km/h), running (9 km/h), walking on a slippery walkway (~2.8 km/h), and backward walking (3 km/h). Mean waveforms for the right (*A*) and left (*B*) legs are plotted vs. the normalized gait cycle (beginning from the foot contact of the right leg). Corresponding right and left cord MN activation patterns (nonnormalized method) are shown on the *bottom* of each panel.

activity is associated with EMG activity in the proximal (thigh) leg muscles and ankle dorsiflexors. It is responsible for braking and weight acceptance at the beginning of stance of each leg and for pulling the contralateral swinging limb forward. During running, there is a similar correspondence. Whereas the temporal locus of the upper lumbar activation is similar (corresponding to EMG activity in the proximal thigh leg muscles and their weight acceptance function), the sacral activation responsible for limb loading at midstance and propulsion is significantly shifted earlier due to the shorter stance phase duration in running. As a result, the sacral CoA has two peaks at 15 and 65% of the gait cycle (Fig. 5*B*, *right*).

Thus the center of MN activity in the lumbosacral enlargement showed two prominent oscillations within one gait cycle on the normal floor (Fig. 5*B*). The intensity of the total lumbosacral MN activation increases with speed of locomotion (Ivanenko et al. 2008). Note, however, that the intensity of activation is a different issue relative to topography. The correlation coefficients between CoA and E_k were 0.94 ± 0.03 and 0.93 ± 0.06, for walking and running, respectively (Fig. 5*B*). E_p also correlated with CoA, since E_p and E_k are interrelated due to the pendulum mechanism (Cavagna et al. 1976; Saibene and Minetti 2003), although the correlation coefficients were slightly lower (−0.83 ± 0.09 and 0.77 ± 0.19 for

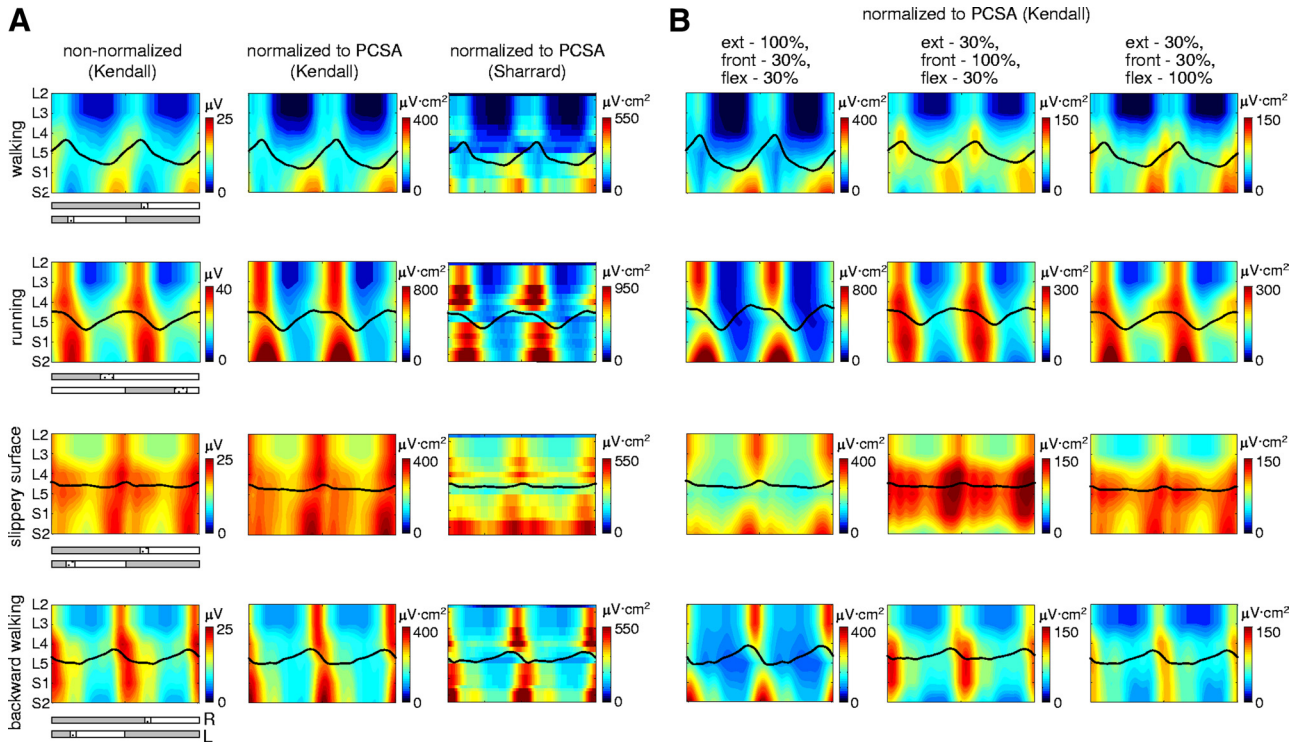

FIG. 4. Parametric sensitivity of the spatiotemporal patterns and the center of bilateral MN activity in the lumbosacral enlargement during different gaits. *A*: 3 different normalization procedures were used to assess parametric sensitivity. *Left*: nonnormalized method (EMGs were expressed in microvolts [μV]) using Kendall's chart. *Middle*: normalized (to physiological cross-sectional area [PCSA]) method using Kendall's chart. *Right*: normalized method using Sharrard's chart. Color scale denotes relative amplitude. Positions of the center of mass of MN activity (center of activity [CoA]) were calculated at each time of the step cycle (black curves). *B*: variations in assumed activation patterns to assess parametric sensitivity (normalized-to-PCSA method using Kendall's chart). Three parametric variations are illustrated by altering the relative level of MN recruitment in leg muscles with the dominant action as extensors (SOL, LG, MG, VL, VM, RF, GM), frontal plane muscles (ADD, TFL, Gmed, SART, PERL) and flexors (TA, ST, BF). 100% corresponds to "no alteration," 30% corresponds to a decreased contribution of a particular muscle group (EMGs were multiplied by 0.3). Note similar CoA behavior when using different normalization techniques. ADD, adductor longus; BF, biceps femoris (long head); GM, gluteus maximus; Gmed, gluteus medius; LG, gastrocnemius lateralis; MG, gastrocnemius medialis; PERL, peroneus longus; RF, rectus femoris; SART, sartorius; ST, semitendinosus; SOL, soleus; TA, tibialis anterior; TFL, tensor fascia latae; VL, vastus lateralis; VM, vastus medialis.

walking and running, respectively). In sum, the spatiotemporal CoA shifts mirrored changes in the kinetic and potential energies of the center of mass in the two main gaits.

Figure 6 illustrates changes in the mechanical energy of the COM and the spatiotemporal activation pattern in other gaits. During walking on the slippery surface, the vertical variation of the COM (and E_p, respectively) was similar to that on the nonslippery floor (Fig. 6*A*). However, the exchange between E_p and E_k was much lower because kinetic energy did not show any systematic oscillation over gait cycle due to the reduced horizontal shear forces. Rostral and caudal shifts of the CoA were much smaller than those for normal walking. In addition, the loci of activation were wider and stronger on the slippery surface. It is also worth noting that unilateral maps of activation revealed a high level of activity in all lumbosacral segments throughout the stance phase, but they also did not demonstrate notable rostrocaudal displacements of the CoA (Fig. 3, *third panel*; see also Cappellini et al. 2010). Accordingly, the correlation coefficients between CoA and E_k and E_p (Fig. 6*A*) were low: 0.08 $\pm$ 0.29 and -0.30 ± 0.38, respectively. During backward walking (Fig. 6*B*), the CoA also had two peaks, as in the case of forward walking, although the temporal sequence of sacral and lumbar MN activation was opposite basically because of an opposite activation of leg extensors during weight acceptance and propulsion in backward walking (Fig. 3). Correlation coefficients between CoA and E_k and E_p were -0.83 ± 0.05 and 0.68 ± 0.18, respectively.

To assess whether the anatomical topography weighting in the calculations is in any way important in the CoA patterning that was derived and its degree of correlation to E_k, we also performed an additional analysis based on the assumption that periodic changes of bilateral CoA could perhaps result from a simple alternation of flexor–extensor output activity of the half-center pattern generators (Orlovsky et al. 1999), independent of topography. To this end, hypothetical bilateral CoA measures were obtained by lumping limb extensor (SOL, LG, MG, VL, VM, RF, GM) pools together at one end of the range of segments and flexors (TA, ST, BF) at the other end. This operation means that there are in effect only two scalar variables varying (flexor net activity and extensor net activity), one varying in segment 1 and one in segment 6 with nothing between (Fig. 7). A CoA was calculated accordingly, using *Eqs. 4* and *5*. There is no spatial "wave" or "migration" in the simple analysis suggested, simply some alternation. Although this examination showed some systematic gait-dependent oscillations of activity, these oscillations weakly correlated to E_k. For instance, for the nonnormalized method (Fig. 7, *left column*), $r = 0.58$, 0.23, -0.02, and 0.09 for walking, running, slippery surface, and backward walking, respectively, and for

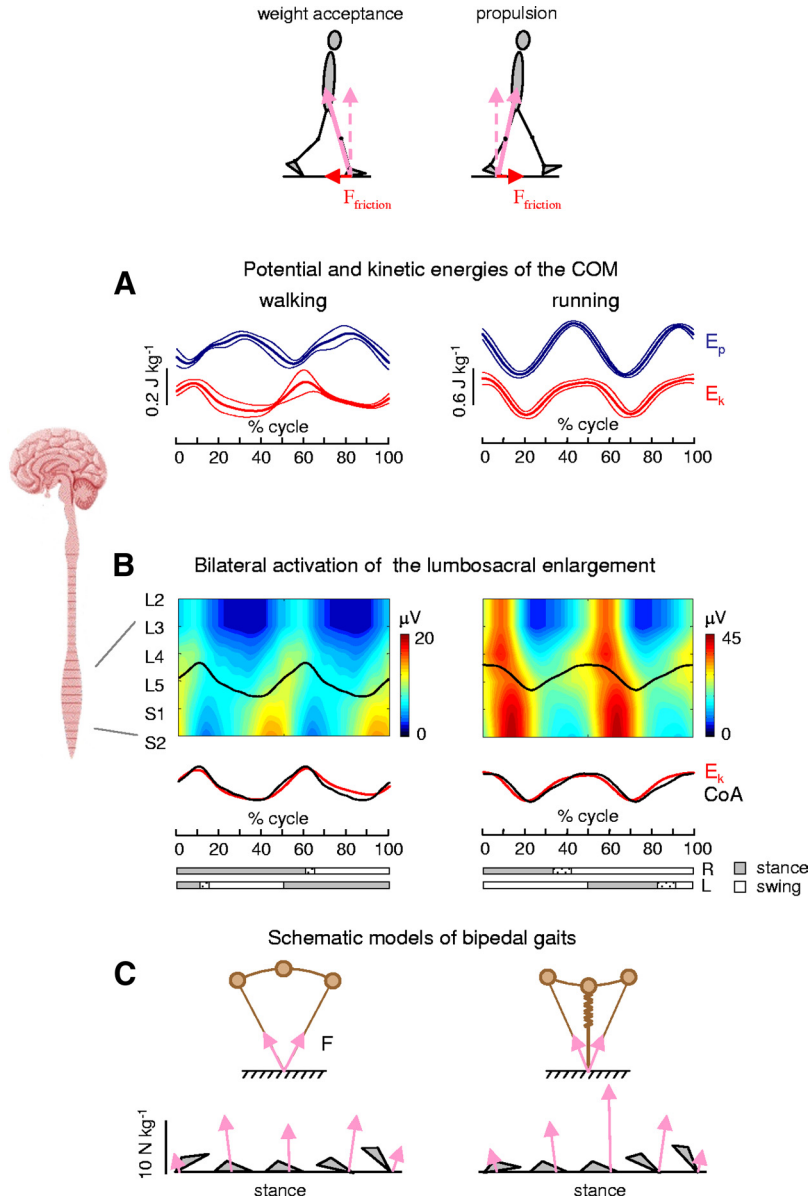

FIG. 5. Total bilateral motor output and center-of-body-mass (COM) motion in human gaits. *A*: potential and kinetic energies (±SD) of the COM during walking and running averaged across subjects. *B*: total bilateral spatiotemporal activation of the lumbosacral enlargement obtained from averaged EMG recordings. Output pattern for each segment was reconstructed by mapping the recorded EMG waveforms (nonnormalized method; Ivanenko et al. 2006) onto the known charts of segmental localization. Pattern is plotted vs. normalized gait cycle in a color scale using a filled contour plot. The black curves correspond to the center of MN activity (CoA), which is superimposed on the COM kinetic energy curves on the *bottom*. Note systematic oscillations of the CoA from S1 to L4 segments (twice per stride) during both walking and running. *C*: schematic representation of different gaits (*top panels*) and general foot placement and contact force characteristics (*bottom panels*). Foot orientation and ground reaction forces (upward pointing vectors) are illustrated in 5 discrete moments of the stance phase in one representative subject.

the normalized-to-PCSA method (Fig. 7, *right column*), r = 0.64, 0.24, −0.05, and 0.09. Thus this "simpler" CoA was not as good at matching and correlating to the E_k as that of the "topographical" CoA calculations (Figs. 5 and 6).

DISCUSSION

In general, activity patterns during different gaits consist of distinct bursts of activity linked to liftoff and touchdown events (Cappellini et al. 2006; Giszter et al. 2007; Ivanenko et al. 2008). We used the EMG data to construct maps of spinal MN activity by adding up the contributions of each muscle to the total activity in each spinal segment. The maps cover spinal levels L2–S2, corresponding to the levels of the MNs innervating the 30 recorded bilateral muscles. Since COM motion of the body is determined by coordinated activity of all muscles of both legs rather than by muscles of only one leg, we attempted to correlate the total spatiotemporal pattern of MN activity with the potential and kinetic energies of the COM in different human gaits. The obtained result (Fig. 5) is not a trivial finding since a priori one might expect various possible solutions for the CoA behavior. For instance, based on the previous studies on fundamental patterns of bilateral muscle activity in human locomotion (Ivanenko et al. 2004; Olree and Vaughan 1995), one might expect four or five oscillations of the CoA (corresponding to the basic temporal EMG components) or even a more complex bilateral MN pattern. However, the results demonstrated only two prominent oscillations within one gait cycle and, furthermore, these spatiotemporal CoA shifts mirrored changes in the kinetic and potential energies of the center of mass in the two main gaits (Fig. 5).

Limitations of the mapping procedure

Analysis of the spatiotemporal pattern of α-MN activity during locomotion is based on several assumptions. MN activation was assessed by mapping the activity patterns from a large number of simultaneously recorded muscles onto the

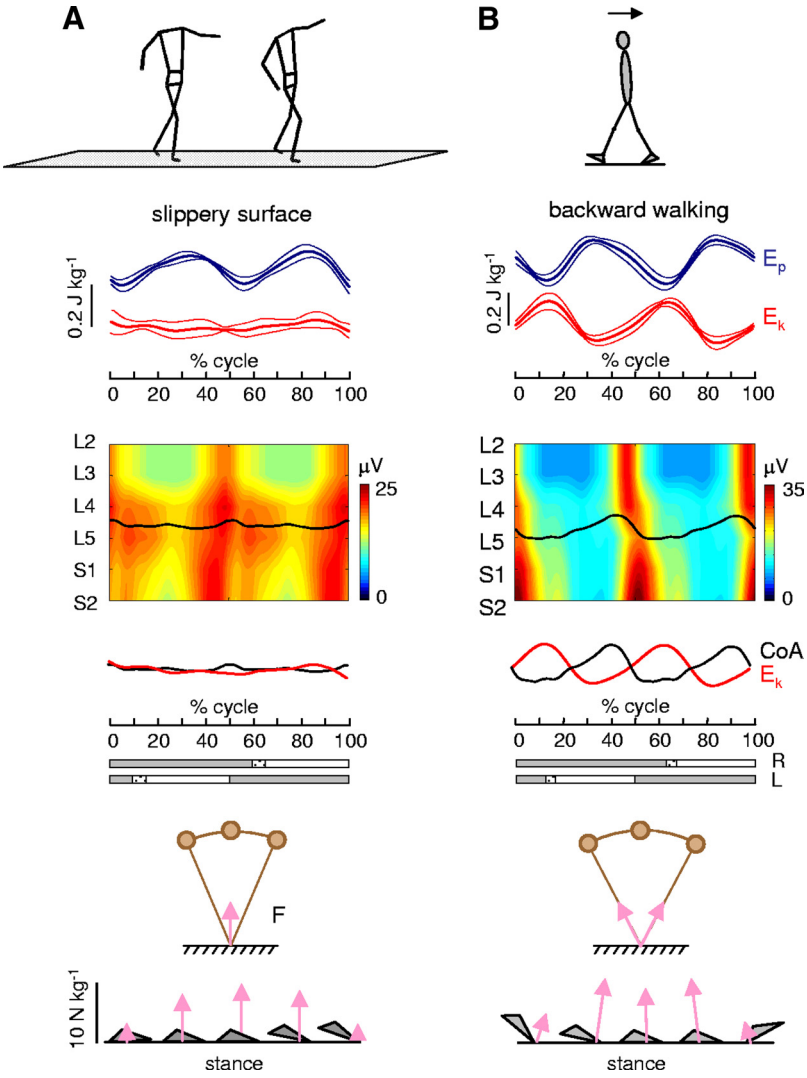

FIG. 6. Total bilateral motor output and changes in the mechanical energy of the COM during walking on a slippery walkway and backward walking on a treadmill at 3 km/h. The same format as that in Fig. 5, *A* and *B*.

approximate rostrocaudal location of the MN pools in the human spinal cord. First, the implicit assumption is that the rectified EMG provides an indirect measure of the net firing of MNs of that muscle. Second, we assumed that our population of subjects has the same spinal topography as that of the reference population (Kendall et al. 1993). In this regard, it should be noted that, despite likely anatomical variability, the data from these charts appear sufficiently robust for the spatial resolution currently available. Third, the CoA can be considered as an approximate approach only because averaging between distinct foci of activity (for instance, L2 and S2) may lead to misleading activity in the midsegments (~L5). Finally, we recorded only a subset of leg muscles.

Nevertheless, the results basically did not change when we used different normalization procedures (Fig. 4), indicating that the functional topography of spinal cord activation is sufficiently robust so far as it concerns rostrocaudal migration of motor pool activity (the time course of the CoA oscillations). On the other hand, simple alternations of flexor–extensor activity were not as good at matching and correlating to the E_k (Fig. 7) as the "topographical" CoA calculations (Figs. 5 and 6). This was likely not only because flexor and extensor motor pools are largely overlapped but also because different extensor groups are "functionally" distributed in the lumbosacral enlargement (Table 1, Fig. 1). It is also worth noting that parametric variations in the relative level of MN recruitment of extensor, flexor, and retractor muscles may change the relative intensity of segmental activation, although the rostrocaudal detour of the center of activity is still very similar (Yakovenko et al. 2002). Furthermore, although we recorded only a subset of leg muscles, the resulting behavior of the CoA was similar when we eliminated any one of the recorded muscles, probably because the lumbosacral enlargement innervates numerous muscles. In fact, even when using intramuscular recordings or when a slightly different set of muscle recordings was used to generate the maps during walking (Ivanenko et al. 2006, 2008), both the maps and the basic bursts of the MN activity were strikingly similar. In sum, the general features of the rostrocaudal shift of the center of bilateral activity seem to be preserved, independently of the normalization procedure (Fig. 4). Moreover, these features correlate nicely with the changes in the energy of the COM motion during bipedal gait (Figs. 5 and 6).

Functional topography of the spinal cord activation in different human gaits

What is special in the biomechanics of human gait? A unique feature of human bipedal gait is the heel-to-toe rolling pattern during the stance phase. As a result of this transfer of

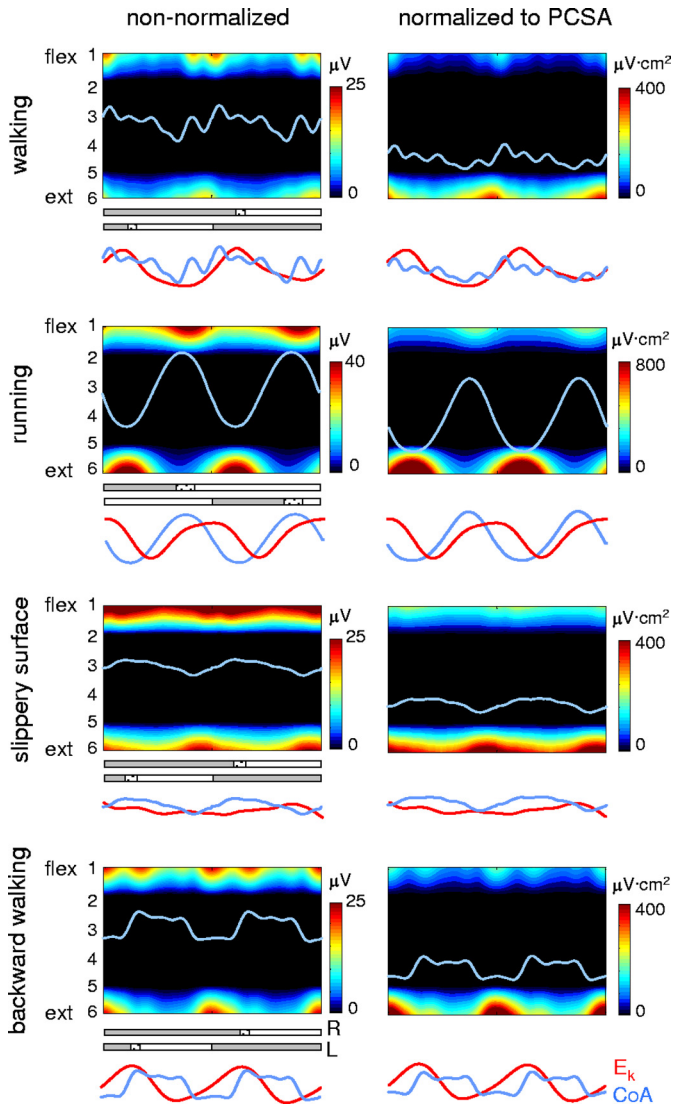

FIG. 7. Motor pool topography weighting vs. "flexor–extensor" CoA alternation. Hypothetical bilateral CoA measures were obtained by lumping limb extensors (SOL, LG, MG, VL, VM, RF, GM) pools together at one end of the range of segments (segment 6) and flexors (TA, ST, BF) at the other end (segment 1). Both nonnormalized and normalized-to-PCSA methods were used. Note weak correspondence of these CoA oscillations to kinetic energy (E_k), as opposed to "topographical" CoA computations in Figs. 5 and 6.

the center of pressure, the ground reaction force vector at touchdown (weight acceptance) passes close to the ankle joint and thus does not require any ankle torque (Fig. 5, *top*). In contrast, during propulsion, when the center of pressure is close to the toe, the propulsion force vector does not cross the ankle joint, requiring an ankle torque that is generated by the distal extensors. Thus the extensor muscles activated by sacral MN are mostly active during propulsion and silent during weight acceptance. The opposite pattern is seen for the proximal extensors activated by lumbar MNs. These muscles produce a hip and knee torque during weight acceptance and are mostly silent during propulsion. The result of this kinematic pattern is that the center of MN activity (CoA) in the spinal cord oscillates between the sacral and lumbar segments over the step cycle. The situation is somewhat similar during running except that the stance phase is relatively shorter. In this case the ground reaction force at touchdown still passes near the ankle as weight acceptance is taken up near mid foot and the propulsion occurs from the toes requiring torque at the ankle.

The friction forces during locomotion also oscillate between a negative (backward directed) force at touchdown and a positive (forward directed) force in propulsion (Fig. 5, *top*). The backward friction force at touchdown reduces E_k and it is resisted by proximal extensors. The propulsive force generated by distal extensors increases E_k and opposes the forward directed friction force. In this way the changes in E_k are correlated with the changes in muscle activation between proximal and distal extensors (Fig. 5*B*). According to this analysis one would expect that in the absence of frictional forces, the kinetic energy would not show such oscillations nor would the CoA have a corresponding trajectory. Even though the CoA may be regulated by more factors than the energy of COM motion as the locomotor task becomes more challenging, both the CoA and E_k oscillations nevertheless reduced in parallel during walking on a slippery surface. Indeed, the E_k is nearly constant over the step cycle (Fig. 6*A*, top) because there are only minor net braking or propulsive forces (Cappellini et al. 2010). Moreover, despite the oscillations of MN activity in both the lumbar and sacral segments, there was no net dominance of one area over the other during the step cycle (Fig. 6*A*).

The fact that the CoA and E_k (rather than E_p) oscillations reduced in parallel on the slippery surface may likely point toward the major contribution of E_k to the CoA. One may also mention the always positive correlation of E_k with CoA during walking and running, whereas for E_p it is negative during walking (Fig. 5*A*). Therefore one might hypothesize that the rostrocaudal CoA shifts are linked more to E_k rather than to E_p. Since E_k oscillations during walking result mainly from changes in the horizontal COM velocity (Cavagna et al. 1976; Tesio et al. 1998), due to alternating horizontal shear forces at the beginning and end of stance, this makes an interesting prediction concerning the sign of correlation between E_k and CoA: that is, during backward walking the direction of shear forces is basically opposite to that of forward walking (Fig. 6*B*, *bottom*) and may thus affect the sign of correlation. Indeed, during backward walking the dominance of sacral and lumbar MN activation is opposite relative to that during forward walking, yet the changes in kinetic energy are still similar (Fig. 6*B*). In this case the touchdown occurs with the toes and the weight acceptance force vector is directed across the ankle joint with ankle torque bearing the load. Similarly at liftoff the propulsion is exerted through the heel with no net torque at the ankle. Once again E_k is positive at liftoff and negative at midstance, but in this case the distal extensors are active at the beginning of stance and the proximal extensors show activity at the end of stance. This would lead to opposite trajectories for the CoA and the E_k, as shown in Fig. 6*B*.

In sum we reported for the first time that the major features of bipedal gait mechanics are reflected in the rostrocaudal propagation of spinal cord activity (Fig. 5). Motor pool spatial organization is likely a developmental outcome of fairly ancient lineage rather than a structural basis of computation, although conceivably these are interrelated and they may reflect basic functioning of leg muscles during terrestrial locomotion. Comparative studies on the organization of spinal motor output in different animal species with regard to their

gaits may shed light on the underlying principles of evolutionary adopted MN grouping and motor wave propagation in the spinal cord (Alexander 1989; Bramble and Lieberman 2004; Clarac et al. 2004; Courtine et al. 2005; Falgairolle et al. 2006; Giszter et al. 2010; Orlovsky et al. 1999).

GRANTS

This work was supported by Italian Health Ministry, Italian University Ministry (PRIN project), Italian Space Agency (CRUSOE grant), and European Union FP7 Information and Communication Technologies Program MINDWALKER Grant 247959 and Adaptive Modular Architectures for Rich Motor Skills Grant 248311.

DISCLOSURES

No conflicts of interest, financial or otherwise, are declared by the authors.

REFERENCES

Alexander RM. Optimization and gaits in the locomotion of vertebrates. *Physiol Rev* 69: 1199–1227, 1989.

Bianchi L, Angelini D, Lacquaniti F. Individual characteristics of human walking mechanics. *Pflügers Arch* 436: 343–356, 1998.

Bonnot A, Whelan PJ, Mentis GZ, O'Donovan MJ. Spatiotemporal pattern of motoneuron activation in the rostral lumbar and the sacral segments during locomotor-like activity in the neonatal mouse spinal cord. *J Neurosci* 22: RC203, 2002.

Bramble DM, Lieberman DE. Endurance running and the evolution of Homo. *Nature* 432: 345–352, 2004.

Cappellini G, Ivanenko YP, Dominici N, Poppele RE, Lacquaniti F. Motor patterns during walking on a slippery walkway. *J Neurophysiol* 103: 746–760, 2010.

Cappellini G, Ivanenko YP, Poppele RE, Lacquaniti F. Motor patterns in human walking and running. *J Neurophysiol* 95: 3426–3437, 2006.

Cavagna GA, Thys H, Zamboni A. The sources of external work in level walking and running. *J Physiol* 262: 639–657, 1976.

Clarac F, Brocard F, Vinay L. The maturation of locomotor networks. *Prog Brain Res* 143: 57–66, 2004.

Courtine G, Roy RR, Hodgson J, McKay H, Raven J, Zhong H, Yang H, Tuszynski MH, Edgerton VR. Kinematic and EMG determinants in quadrupedal locomotion of a non-human primate (Rhesus). *J Neurophysiol* 93: 3127–3145, 2005.

Cuellar CA, Tapia JA, Juarez V, Quevedo J, Linares P, Martinez L, Manjarrez E. Propagation of sinusoidal electrical waves along the spinal cord during a fictive motor task. *J Neurosci* 29: 798–810, 2009.

de Sèze M, Falgairolle M, Viel S, Assaiante C, Cazalets JR. Sequential activation of axial muscles during different forms of rhythmic behavior in man. *Exp Brain Res* 185: 237–247, 2008.

Dostal WF, Soderberg GL, Andrews JG. Actions of hip muscles. *Phys Ther* 66: 351–361, 1986.

Falgairolle M, de Sèze M, Juvin L, Morin D, Cazalets JR. Coordinated network functioning in the spinal cord: an evolutionary perspective. *J Physiol (Paris)* 100: 304–316, 2006.

Giszter S, Patil V, Hart C. Primitives, premotor drives, and pattern generation: a combined computational and neuroethological perspective. *Prog Brain Res* 165: 323–346, 2007.

Giszter SF, Hart CB, Silfies SP. Spinal cord modularity: evolution, development, and optimization and the possible relevance to low back pain in man. *Exp Brain Res* 200: 283–306, 2010.

Golubitsky M, Stewart I, Buono PL, Collins JJ. Symmetry in locomotor central pattern generators and animal gaits. *Nature* 401: 693–695, 1999.

Grillner S. Biological pattern generation: the cellular and computational logic of networks in motion. *Neuron* 52: 751–766, 2006.

Ivanenko YP, Cappellini G, Poppele RE, Lacquaniti F. Spatiotemporal organization of alpha-motoneuron activity in the human spinal cord during different gaits and gait transitions. *Eur J Neurosci* 27: 3351–3368, 2008.

Ivanenko YP, Dominici N, Lacquaniti F. Development of independent walking in toddlers. *Exerc Sport Sci Rev* 35: 67–73, 2007.

Ivanenko YP, Poppele RE, Lacquaniti F. Five basic muscle activation patterns account for muscle activity during human locomotion. *J Physiol* 556: 267–282, 2004.

Ivanenko YP, Poppele RE, Lacquaniti F. Spinal cord maps of spatiotemporal alpha-motoneuron activation in humans walking at different speeds. *J Neurophysiol* 95: 602–618, 2006.

Ivanenko YP, Poppele RE, Lacquaniti F. Distributed neural networks for controlling human locomotion: lessons from normal and SCI subjects. *Brain Res Bull* 78: 13–21, 2009.

Kendall FP, Provance PG, McCreary EK. *Muscles: Testing and Function with Posture and Pain* (4th ed.). Baltimore, MD: Williams & Wilkins, 1993.

Lacquaniti F, Grasso R, Zago M. Motor patterns in walking. *News Physiol Sci* 14: 168–174, 1999.

Lacquaniti F, Ivanenko YP, Zago M. Kinematic control of walking. *Arch Ital Biol* 140: 263–272, 2002.

Massaad F, Lejeune TM, Detrembleur C. The up and down bobbing of human walking: a compromise between muscle work and efficiency. *J Physiol* 582: 789–799, 2007.

Mentel T, Cangiano L, Grillner S, Buschges A. Neuronal substrates for state-dependent changes in coordination between motoneuron pools during fictive locomotion in the lamprey spinal cord. *J Neurosci* 28: 868–879, 2008.

Nilsson J, Thorstensson A, Halbertsma J. Changes in leg movements and muscle activity with speed of locomotion and mode of progression in humans. *Acta Physiol Scand* 123: 457–475, 1985.

Olree KS, Vaughan CL. Fundamental patterns of bilateral muscle activity in human locomotion. *Biol Cybern* 73: 409–414, 1995.

Orlovsky GN, Deliagina TG, Grillner S. *Neural Control of Locomotion. From Mollusc to Man*. Oxford, UK: Oxford Univ. Press, 1999.

Saibene F, Minetti AE. Biomechanical and physiological aspects of legged locomotion in humans. *Eur J Appl Physiol* 88: 297–316, 2003.

Sharrard WJW. The segmental innervation of the lower limb muscles in man. *Ann R Coll Surg Engl* 35: 106–122, 1964.

Srinivasan M, Ruina A. Computer optimization of a minimal biped model discovers walking and running. *Nature* 439: 72–75, 2006.

Tesio L, Lanzi D, Detrembleur C. The 3-D motion of the centre of gravity of the human body during level walking. I. Normal subjects at low and intermediate walking speeds. *Clin Biomech* 13: 77–82, 1998.

Ward SR, Eng CM, Smallwood LH, Lieber RL. Are current measurements of lower extremity muscle architecture accurate? *Clin Orthop Relat Res* 467: 1074–1082, 2009.

Yakovenko S, Mushahwar V, VanderHorst V, Holstege G, Prochazka A. Spatiotemporal activation of lumbosacral motoneurons in the locomotor step cycle. *J Neurophysiol* 87: 1542–1553, 2002.